

# Statistical Properties of Nonlinear Phase Noise

Keang-Po Ho

*StrataLight Communications, Campbell, CA 95008\**

(Dated: February 9, 2020)

The statistical properties of nonlinear phase noise, often called the Gordon-Mollenauer effect, is studied analytically when the number of fiber spans is very large. The joint characteristic functions of the nonlinear phase noise with electric field, received intensity, and the phase of amplifier noise are all derived analytically. Based on the joint characteristic function of nonlinear phase noise with the phase of amplifier noise, the error probability of signal having nonlinear phase noise is calculated using the Fourier series expansion of the probability density function. The error probability is increased due to the dependence between nonlinear phase noise and the phase of amplifier noise. When the received intensity is used to compensate the nonlinear phase noise, the optimal linear and nonlinear compensators are derived analytically using the joint characteristic function of nonlinear phase noise and received intensity. The nonlinear compensator based on the conditional mean performs slightly better than the linear compensator.

PACS numbers: 42.65.-k, 05.40.-a, 42.79.Sz, 42.81.Dp

Keywords: Nonlinear phase noise, Fiber nonlinearities, Noise statistics

## I. INTRODUCTION

When optical amplifiers are used to compensate for fiber loss, the interaction of amplifier noise and the fiber Kerr effect causes phase noise, often called the Gordon-Mollenauer effect or nonlinear phase noise [1]. Nonlinear phase noise degrades phase-modulated signal like phase-shifted keying (PSK) and differential phase-shift keying (DPSK) signal [1, 2, 3, 4, 5, 6, 7, 8]. This class of constant-intensity modulation has renewed attention recently for long haul and/or spectral efficiency transmission systems [9, 10, 11, 12, 13, 14, 15].

Traditionally, the performance of the system is evaluated based on the variance of the nonlinear phase noise [1, 4, 5, 6, 7]. Recently, it is found that the nonlinear phase noise is not Gaussian-distributed both experimentally [8] and analytically [16, 17]. For non-Gaussian noise, neither the variance nor the  $Q$ -factor is sufficient to characterize the performance of the system. The probability density function (p.d.f.) is required to better understand the noise properties and evaluates the system performance.

The p.d.f. of nonlinear phase noise alone [16, 17] is not sufficient to characterize the signal with nonlinear phase noise. Because of the dependence between nonlinear phase noise and signal phase, the joint p.d.f. of the nonlinear phase noise and the signal phase is required to evaluate the error probability for a phase-modulated system. This article provides analytical expressions of the joint asymptotic characteristic functions for the nonlinear phase noise and the received electric field without nonlinear phase noise. The amplifier noise is asymptotically modeled as a distributed process for a large number of fiber spans. After the characteristic function is

first derived analytically, the p.d.f. is the inverse Fourier transform of the corresponding characteristic function.

The received phase is the summation of the nonlinear phase noise and the phase of amplifier noise. Using the joint characteristic function of nonlinear phase noise and the phase of amplifier noise, the p.d.f. of the received phase can be expanded as a Fourier series. Using the Fourier series, the error probability of DPSK signal is evaluated by a series summation. Because the nonlinear phase noise has a weak dependence on the phase of amplifier noise, the Fourier series expansion is more complicated than traditional method in which the extra phase noise is independent of the signal phase [18, 19].

Correlated with each other, the received intensity can be used to compensate the nonlinear phase noise. When a linear compensator compensates the nonlinear phase noise using a scaled version of the received intensity [5, 6, 7, 20], the optimal linear compensator is found using the joint characteristic function of nonlinear phase noise and received intensity. The minimum mean-square compensator is the conditional mean of the nonlinear phase noise given the received intensity [21, §10.2]. Using the conditional characteristic function of the nonlinear phase noise given the received intensity, the optimal nonlinear compensator is found to perform slightly better than the linear compensator.

Sec. II builds the mathematical model of the nonlinear phase noise and derives the joint characteristic function of the normalized nonlinear phase noise and electric field. Sec. III gives the marginal p.d.f. of nonlinear phase noise by inverse Fourier transform. Sec. IV obtains the joint characteristic functions of the nonlinear phase noise with received intensity and the phase of amplifier noise. Using the joint characteristic function of nonlinear phase noise with the phase of amplifier noise, Sec. V calculates the exact error probability of DPSK signal with nonlinear phase noise. An approximation is also presented based on the assumption that the nonlinear phase noise is indepen-

---

\*Electronic address: kpho@stratalight.com

dent of the phase of amplifier noise. Using the joint characteristic function of nonlinear phase noise with received intensity, Sec. VI provides the optimal linear and nonlinear compensators to compensate the nonlinear phase noise using received intensity. Finally, Sec. VII is the conclusion of this article.

## II. JOINT STATISTICS OF NONLINEAR PHASE NOISE AND ELECTRIC FIELD

This section provides the joint characteristic function of nonlinear phase noise and the electric field without nonlinear phase noise. Both the nonlinear phase noise and the electric field are first normalized and represented as the summation of infinite number of independently distributed random variables. The joint characteristic function of nonlinear phase noise and electric field is the product of the corresponding joint characteristic functions of those random variables. After some algebraic simplifications, the joint characteristic function has a simple expression.

### A. Normalization of Nonlinear Phase Noise

In a lightwave system, nonlinear phase noise is induced by the interaction of fiber Kerr effect and optical amplifier noise. In this article, nonlinear phase noise is induced by self-phase modulation through the amplifier noise in the same polarization as the signal and within an optical bandwidth matched to the signal. The phase noise induced by cross-phase modulation from amplifier noise outside that optical bandwidth is ignored for simplicity. The amplifier noise from the orthogonal polarization is also ignored for simplicity. As shown later, we can include the phase noise from cross-phase modulation or orthogonal polarization by simple modification.

For an  $N$ -span fiber system, the overall nonlinear phase noise is [1] [7] [16]

$$\phi_{\text{NL}} = \gamma L_{\text{eff}} \left\{ |\vec{E}_0 + \vec{n}_1|^2 + |\vec{E}_0 + \vec{n}_1 + \vec{n}_2|^2 + \dots + |\vec{E}_0 + \vec{n}_1 + \dots + \vec{n}_N|^2 \right\}, \quad (1)$$

where  $\vec{E}_0$  is a two-dimensional vector as the baseband representation of the transmitted electric field,  $\vec{n}_k, k = 1, \dots, N$ , are independent identically distributed (i.i.d.) zero-mean circular Gaussian random vectors as the optical amplifier noise introduced into the system at the  $k^{\text{th}}$  fiber span,  $\gamma L_{\text{eff}}$  is the product of fiber nonlinear coefficient and the effective fiber length per span. In (1), both electric field of  $\vec{E}_0$  and amplifier noises of  $\vec{n}_k$  can also be represented as a complex number.

Figs. 1 show the simulated distribution of the received electric field including the contribution from nonlinear phase noise. The mean nonlinear phase shifts  $\langle \Phi_{\text{NL}} \rangle$

are 1 and 2 rad for Figs. 1a and 1b, respectively. The mean nonlinear phase shift of  $\langle \Phi_{\text{NL}} \rangle = 1$  rad corresponds to the limitation estimated by [1]. The mean nonlinear phase shift of  $\langle \Phi_{\text{NL}} \rangle = 2$  rad corresponds to the limitation given by [7] when the standard deviation of nonlinear phase noise is halved using a linear compensator.

Figs. 1 are plotted for the case that the signal-to-noise ratio (SNR)  $\rho_s = 18$ , corresponding to an error probability of  $10^{-9}$  if the amplifier noise is the sole impairment. The number of spans is  $N = 32$ . The transmitted signal is  $\vec{E}_0 = (\pm |\vec{E}_0|, 0)$  for binary PSK system. The distribution of Figs. 1 has 5000 points for different noise combinations. In practice, the signal distribution of Figs. 1 can be measured using an optical phase-locked loop (see Fig. 5 of [22]). Note that although the optical phase-locked loop actually tracks out the mean nonlinear phase shift of  $\langle \Phi_{\text{NL}} \rangle$ , nonzero values of  $\langle \Phi_{\text{NL}} \rangle$  have been preserved in plotting Figs. 1 to better illustrate the nonlinear phase noise.

With large number of fiber spans, the summation of (1) can be replaced by integration as [5, 17]

$$\phi_{\text{NL}} = \kappa \int_0^L |\vec{E}_0 + \vec{S}(z)|^2 dz, \quad (2)$$

where  $L$  is the overall fiber length,  $\kappa = N\gamma L_{\text{eff}}/L$  is the average nonlinear coefficient per unit length, and  $\vec{S}(z)$  is a zero-mean two-dimensional Brownian motion of  $E\{\vec{S}(z_1) \cdot \vec{S}(z_2)\} = \sigma_s^2 \min(z_1, z_2)$ , where  $\cdot$  denotes inner product of two vectors. The variance of  $\sigma_s^2 = N\sigma_{\text{ASE}}^2/L$  is the noise variance per unit length where  $E\{|\vec{n}_k|^2\} = \sigma_{\text{ASE}}^2, k = 1, \dots, N$  is noise variance per amplifier per polarization in the optical bandwidth matched to the signal.

In this article, we investigate the joint statistical properties of the normalized electric field and normalized nonlinear phase noise

$$\vec{e}_N = \vec{\xi}_0 + \vec{b}(1), \quad \phi = \int_0^1 |\vec{\xi}_0 + \vec{b}(t)|^2 dt, \quad (3)$$

where  $\vec{b}(t)$  is a two-dimensional Brownian motion with an autocorrelation function of

$$R_b(t, s) = E\{\vec{b}(s) \cdot \vec{b}(t)\} = \min(t, s). \quad (4)$$

Comparing the phase noise of (2) and (3), the normalized nonlinear phase noise of (3) is scaled by  $\phi = L\sigma_s^2\phi_{\text{NL}}/\kappa$ ,  $t = z/L$  is the normalized distance,  $b(t) = S(tL)/\sigma_s/\sqrt{L}$  is the normalized amplifier noise,  $\vec{\xi}_0 = \vec{E}_0/\sigma_s/\sqrt{L}$  is the normalized transmitted vector, and the normalized electric field of  $\vec{e}_N$  is scaled by the inverse of the noise variance. The SNR of the signal is  $\rho_s = |\vec{\xi}_0|^2 = |\vec{E}_0|^2/(L\sigma_s^2) = |\vec{E}_0|^2/(N\sigma_{\text{ASE}}^2)$ .

In (3), the normalized electric field  $\vec{e}_N$  is the normalized received electric field without nonlinear phase noise.

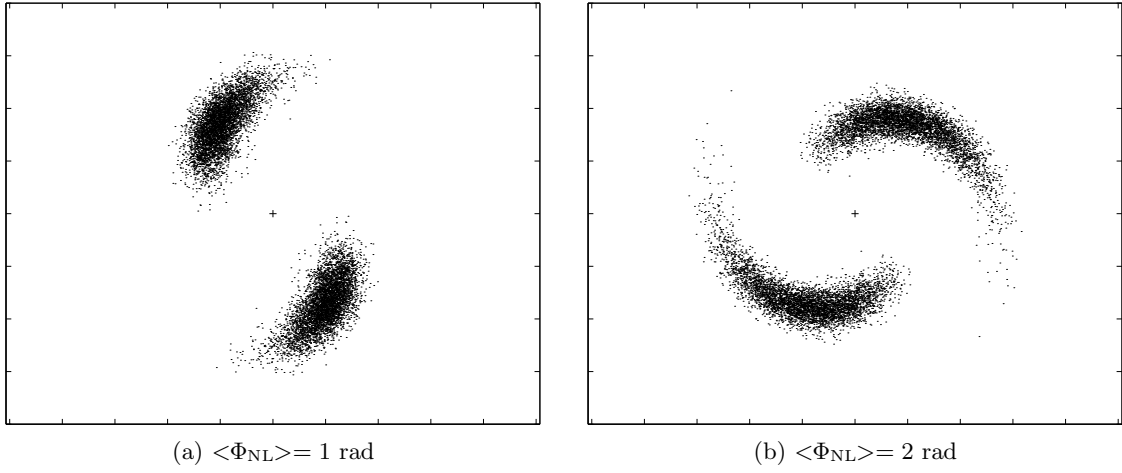


FIG. 1: Simulated distribution of the received electric field for mean nonlinear phase shift of (a)  $\langle \Phi_{NL} \rangle = 1$  rad and (b)  $\langle \Phi_{NL} \rangle = 2$  rad.

The actual normalized received electric field, corresponding to Fig. 1, is  $\vec{e}_r = \vec{e}_N \exp(-j\phi)$ . The actual normalized received electric field has the same intensity as that of the normalized electric field  $\vec{e}_N$ , i.e.,  $|\vec{e}_r|^2 = |\vec{e}_N|^2$ . The values of  $y = |\vec{e}_N|^2$  and  $r = |\vec{e}_N|$  are called normalized received intensity and amplitude, respectively.

### B. Series Expansion

The Brownian motion of  $\vec{b}(t)$  can be expanded using the standard Karhunen-Loève expansion of [23, §10-6]

$$\vec{b}(t) = \sum_{k=1}^{\infty} \sigma_k \vec{x}_k \psi_k(t), \quad (5)$$

where  $\vec{x}_k$  are i.i.d. two-dimensional circular Gaussian random variables with zero mean and unity variance of  $E\{|\vec{x}_k|^2\} = 1$ , the eigenvalues and eigenfunctions of  $\sigma_k^2, \psi_k(t), 0 \leq t \leq 1$  are [17] [23, p. 305]

$$\sigma_k = \frac{2}{(2k-1)\pi}, \psi_k(t) = \sqrt{2} \sin\left[\frac{(2k-1)\pi}{2}t\right]. \quad (6)$$

Substitute (5) with (6) into the normalized phase of (3), because  $\int_0^1 \sin(t/\sigma_k) dt = \sigma_k$ , we get

$$\phi = |\vec{\xi}_0|^2 + 2\sqrt{2} \sum_{k=1}^{\infty} \sigma_k^2 \vec{\xi}_0 \cdot \vec{x}_k + \sum_{k=1}^{\infty} \sigma_k^2 |\vec{x}_k|^2. \quad (7)$$

Because  $\sum_{k=1}^{\infty} \sigma_k^2 = 1/2$  (see [24, §0.234]), we get

$$\phi = \sum_{k=1}^{\infty} \sigma_k^2 |\sqrt{2}\vec{\xi}_0 + \vec{x}_k|^2. \quad (8)$$

The random variable  $|\sqrt{2}\vec{\xi}_0 + \vec{x}_k|^2$  is a noncentral chi-square ( $\chi^2$ ) random variable with two degrees of freedom with a noncentrality parameter of  $2\rho_s$  and a variance parameter of  $1/2$  [25, pp. 41-46]. The normalized nonlinear phase noise is the summation of infinitely many independently distributed noncentral  $\chi^2$ -random variables with two degrees of freedom with noncentrality parameters of  $2\sigma_k^2\rho_s$  and variance parameters of  $\sigma_k^2/2$ . The mean and standard deviation (STD) of the random variables are both proportional to the square of the reciprocal of all odd natural numbers.

Using the series expansion of (5), the normalized electric field is

$$\vec{e}_N = \vec{\xi}_0 + \sqrt{2} \sum_{k=1}^{\infty} (-1)^{k+1} \sigma_k \vec{x}_k. \quad (9)$$

Using [24, §0.232], we get  $\sum_{k=1}^{\infty} (-1)^{k+1} \sigma_k = 1/2$  and

$$\vec{e}_N = \sqrt{2} \sum_{k=1}^{\infty} (-1)^{k+1} \sigma_k (\sqrt{2}\vec{\xi}_0 + \vec{x}_k). \quad (10)$$

The normalized electric field of (10) is a two-dimensional Gaussian-distributed random variable having a mean of  $\vec{\xi}_0$  and variance of  $1/2$ .

The series expansion of (8) and (10) can be used to derive the joint characteristic function of the normalized electric field of  $\vec{e}_N$  and nonlinear phase noise of  $\phi$  in (3).

### C. Joint Characteristic Function

The joint characteristic function of the normalized nonlinear phase noise and the electric field of (3) is

$$\Psi_{\Phi, \vec{E}_N}(\nu, \vec{\omega}) = E\{\exp(j\nu\phi + j\vec{\omega} \cdot \vec{e}_N)\}. \quad (11)$$

First of all, we have

$$E \left\{ \exp \left[ j\nu |\sqrt{2}\vec{\xi}_0 + \vec{x}_k|^2 + j\vec{\omega} \cdot (\sqrt{2}\vec{\xi}_0 + \vec{x}_k) \right] \right\} \\ = \frac{1}{1-j\nu} \exp \left( \frac{2j\nu |\vec{\xi}_0|^2 + \sqrt{2}j\vec{\xi}_0 \cdot \vec{\omega} - |\vec{\omega}|^2/4}{1-j\nu} \right). \quad (12)$$

In the above expression, if  $\vec{\omega} = 0$ , the characteristic function of  $|\sqrt{2}\vec{\xi}_0 + \vec{x}_k|^2$  is

$$\Psi_{|\sqrt{2}\vec{\xi}_0 + \vec{x}_k|^2}(\nu) = \frac{1}{1-j\nu} \exp \left( \frac{2j\nu\rho_s}{1-j\nu} \right) \quad (13)$$

for a noncentral  $\chi^2$ -distribution with mean and variance of  $2\rho_s + 1$  and  $4\rho_s + 1$ , respectively [25, p. 42].

The joint characteristic function of  $\Psi_{\Phi, \vec{E}_N}$  is

$$\Psi_{\Phi, \vec{E}_N}(\nu, \vec{\omega}) = \prod_{k=1}^{\infty} \frac{1}{1-j\nu\sigma_k^2} \\ \times \exp \left[ \frac{2j\nu |\vec{\xi}_0|^2 \sigma_k^2 + 2j(-1)^{k+1} \sigma_k \vec{\xi}_0 \cdot \vec{\omega} - \sigma_k^2 |\vec{\omega}|^2/2}{1-j\nu\sigma_k^2} \right] \quad (14)$$

as the product of the joint characteristic function of the corresponding independently distributed random variables in the series expansion of (8) and (10).

Using the expressions of [24, §1.431, §1.421, §1.422]

$$\cos x = \prod_{k=1}^{\infty} \left( 1 - \frac{4x^2}{(2k-1)^2\pi^2} \right), \\ \tan \frac{\pi x}{2} = \frac{4x}{\pi} \sum_{k=1}^{\infty} \frac{1}{(2k-1)^2 - x^2}, \\ \sec \frac{\pi x}{2} = \frac{4}{\pi} \sum_{k=1}^{\infty} \frac{(-1)^{k+1}(2k-1)}{(2k-1)^2 - x^2},$$

the characteristic function of (14) can be simplified to

$$\Psi_{\Phi, \vec{E}_N}(\nu, \vec{\omega}) = \sec \sqrt{j\nu} \\ \times \exp \left[ \left( |\vec{\xi}_0|^2 \sqrt{j\nu} - \frac{|\vec{\omega}|^2}{4\sqrt{j\nu}} \right) \tan \sqrt{j\nu} \right. \\ \left. + j \sec(\sqrt{j\nu}) \vec{\xi}_0 \cdot \vec{\omega} \right]. \quad (15)$$

The trigonometric function with complex argument is calculated by, for example,  $(\sec \sqrt{j\nu})^{-1} = \cos \sqrt{\nu/2} \cosh \sqrt{\nu/2} - j \sin \sqrt{\nu/2} \sinh \sqrt{\nu/2}$ .

The p.d.f. of  $p_{\Phi, \vec{E}_N}(\phi, \vec{z})$  is the inverse Fourier transform of the characteristic function  $\Psi_{\Phi, \vec{E}_N}(\nu, \vec{\omega})$  of (15).

So far, there is no analytical expression for the p.d.f. of  $p_{\Phi, \vec{E}_N}(\phi, \vec{z})$ .

It is also obvious that

$$\Psi_{\vec{E}_N}(\vec{\omega}) = \Psi_{\Phi, \vec{E}_N}(0, \vec{\omega}) = \exp \left( j\vec{\xi}_0 \cdot \vec{\omega} - \frac{|\vec{\omega}|^2}{4} \right) \quad (16)$$

is the characteristic function of a two-dimensional Gaussian distribution [25, pp. 48-51] for the normalized electric field of (10)

The approach here to derive the joint characteristic function of normalized nonlinear phase noise and electric field is similar to that of [26] to find the joint characteristic function for polarization-mode dispersion [27] by using an explicit solution. Another approach is to solve the Fokker-Planck equation of the corresponding diffusion process [23, §12.4].

### III. THE PROBABILITY DENSITY FUNCTION OF NONLINEAR PHASE NOISE

The characteristic function of the normalized nonlinear phase noise is  $\Psi_{\Phi, \vec{E}_N}(\nu, 0)$  or [17]

$$\Psi_{\Phi}(\nu) = \sec \sqrt{j\nu} \exp \left[ \rho_s \sqrt{j\nu} \tan \sqrt{j\nu} \right]. \quad (17)$$

From the characteristic function of (17), the mean normalized nonlinear phase shift is

$$\langle \Phi \rangle = -j \frac{d}{d\nu} \Psi_{\Phi}(\nu) \Big|_{\nu=0} = \rho_s + \frac{1}{2}. \quad (18)$$

Note that the differentiation or partial differentiation operation can be handled by most symbolic mathematical software. The scaling from normalized nonlinear phase noise to the nonlinear phase noise of (2) is

$$\phi_{\text{NL}} = \frac{\langle \Phi_{\text{NL}} \rangle}{\rho_s + 1/2} \phi. \quad (19)$$

The second moment of the nonlinear phase noise is

$$\langle \Phi^2 \rangle = - \frac{d^2}{d\nu^2} \Psi_{\Phi}(\nu) \Big|_{\nu=0} = \frac{2}{3} \rho_s + \frac{1}{6} + \left( \rho_s + \frac{1}{2} \right)^2, \quad (20)$$

giving the variance of normalized phase noise as  $\sigma_{\Phi}^2 = 2\rho_s/3 + 1/6$ .

The p.d.f. of the normalized nonlinear phase noise of (3) can be calculated by taking the inverse Fourier transform of the characteristic function of (17). Fig. 2 shows the p.d.f. of the normalized nonlinear phase noise for three different SNR of  $\rho_s = 11, 18$ , and 25, corresponding to about an error probability of  $10^{-6}$ ,  $10^{-9}$ , and  $10^{-12}$ , respectively, when amplifier noise is the only impairment.

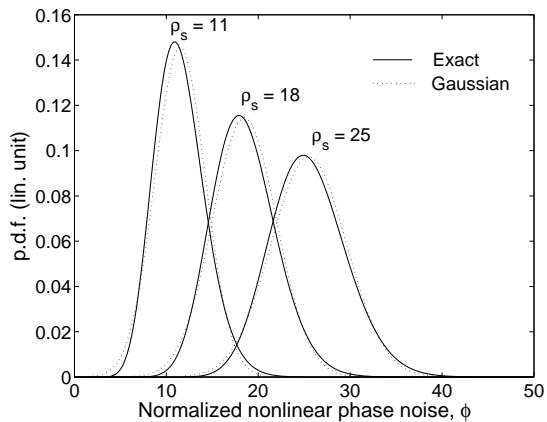


FIG. 2: The p.d.f. of the normalized nonlinear phase noise  $\phi$  for SNR of  $\rho_s = 11, 18,$  and  $25$ .

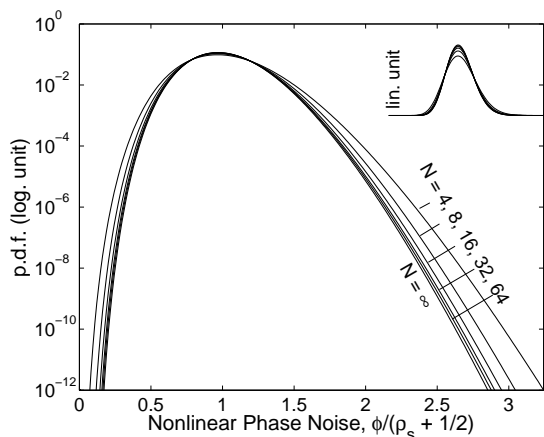


FIG. 3: The asymptotic p.d.f. of normalized nonlinear phase noise of  $\phi$  as compared with the p.d.f. of  $N = 4, 8, 16, 32,$  and  $64$  fiber spans. The p.d.f. in linear scale is shown in the inset.

Fig. 2 shows the p.d.f. using the exact characteristic function (17), and the Gaussian approximation with mean and variance of  $\langle \Phi \rangle = \rho_s + 1/2$  and  $\sigma_\Phi^2 = 2\rho_s/3 + 1/6$ . From Fig. 2, the Gaussian distribution is not a good model for nonlinear phase noise.

The p.d.f. for finite number of fiber spans was derived base on the orthogonalization of the nonlinear phase noise of (1) by the summation of  $N$  independently distributed random variables [16]. Fig. 3 shows a comparison of the p.d.f. for  $N = 4, 8, 16, 32,$  and  $64$  of fiber spans [16] with the asymptotic case of (17). Using the SNR of  $\rho_s = 18$ , Fig. 3 is plotted in logarithmic scale to show the difference in the tail. Fig. 3 also provides an inset in linear scale of the same p.d.f. to show the difference around the mean. The asymptotic p.d.f. of (17) with distributed noise has the smallest spread in the tail as compared with the p.d.f. with  $N$  discrete noise sources. The asymptotic p.d.f. is very accurate for  $N \geq 32$  fiber spans.

As discussed earlier, the effects of amplifier noise outside the signal bandwidth and the amplifier noise from

orthogonal polarization are all ignored for simplicity. If the nonlinear phase noise induced from those amplifier noises is included, based on the simple reasoning of [28], the marginal characteristic function of the normalized nonlinear phase noise of (17) becomes

$$\sec^m \left( \sqrt{j\nu} \right) \exp \left[ \rho_s \sqrt{j\nu} \tan \sqrt{j\nu} \right]. \quad (21)$$

where  $m$  is product of the ratio of the amplifier noise bandwidth to the signal bandwidth and the number of polarizations. If only the amplifier noise from orthogonal polarization matched to signal bandwidth is considered,  $m = 2$  for two polarizations. The mean and variance of the nonlinear phase noise increase slightly to  $\rho_s + m/2$  and  $2\rho_s/3 + m/6$ , respectively. The nonlinear phase noise is induced mainly by the beating of the signal and amplifier noise from the same polarization, similar to the case of signal-spontaneous beat noise in an amplified receiver. For high SNR of  $\rho_s$ , it is obvious that the signal-amplifier noise beating is the major contribution to nonlinear phase noise. The parameter of  $m$  can equal to  $1/2$  for the case if the amplifier noise from another dimension is ignored by confining to single-dimensional signal and noise. In later part of this article, the characteristic function of (17) can be changed to (21) if necessary.

#### IV. SOME JOINT CHARACTERISTIC FUNCTIONS

From (15), we can take the inverse Fourier transform with respect to  $\vec{\omega}$  and get

$$\mathcal{F}_{\vec{\omega}}^{-1} \left\{ \Psi_{\Phi, \vec{E}_N}(\nu, \vec{\omega}) \right\} = \mathcal{F}_{\phi} \left\{ p_{\Phi, \vec{E}_N}(\phi, \vec{z}) \right\}, \quad (22)$$

where  $\mathcal{F}_{\vec{\omega}}^{-1}$  denotes the inverse Fourier transform with respect to  $\vec{\omega}$ , and  $\mathcal{F}_{\phi}$  denotes the Fourier transform with respect to  $\phi$ . The characteristic function of (15) can be rewritten as

$$\Psi_{\Phi, \vec{E}_N}(\nu, \vec{\omega}) = \Psi_{\Phi}(\nu) \exp \left[ - \frac{|\vec{\omega}|^2 \tan \sqrt{j\nu}}{4\sqrt{j\nu}} + j \sec(\sqrt{j\nu}) \vec{\xi}_0 \cdot \vec{\omega} \right]. \quad (23)$$

where  $\Psi_{\Phi}(\nu)$  is the marginal characteristic function of nonlinear phase noise from (17). The inverse Fourier transform is

$$\mathcal{F}_{\vec{\omega}}^{-1} \left\{ \Psi_{\Phi, \vec{E}_N} \right\} = \frac{\Psi_{\Phi}(\nu)}{2\pi\sigma_\nu^2} \exp \left( - \frac{|\vec{z} - \vec{\xi}_\nu|^2}{2\sigma_\nu^2} \right), \quad (24)$$

where  $\sigma_\nu^2 = \tan(\sqrt{j\nu})/(2\sqrt{j\nu})$  and  $\vec{\xi}_\nu = \sec(\sqrt{j\nu})\vec{\xi}_0$ . Both  $\sigma_\nu^2$  and  $\vec{\xi}_\nu$  are complex numbers and can be considered as the angular frequency depending variance and mean, respectively.

### A. Joint Characteristic Function of Nonlinear Phase Noise and Received Intensity

Using the partial p.d.f. and characteristic function of (24), change the random variable from rectangular coordinate of  $\vec{z} = (x, y)$  to polar coordinate of  $\vec{z} = (r \cos \theta, r \sin \theta)$ , we get

$$\mathcal{F}_{\vec{\omega}}^{-1} \{ \Psi_{\Phi, R, \Theta_n} \} = \frac{r \Psi_{\Phi}(\nu)}{2\pi\sigma_{\nu}^2} \times \exp \left[ -\frac{r^2 + |\vec{\xi}_{\nu}|^2 - 2r|\vec{\xi}_{\nu}| \cos(\theta - \theta_0)}{2\sigma_{\nu}^2} \right], \quad (25)$$

where  $\theta_0$  is the angle of the transmitted vector  $\vec{\xi}_0$  and  $|\vec{\xi}_{\nu}| = \sec(\sqrt{j\nu})|\vec{\xi}_0|$ . The random variable of  $\Theta_n$  is called the phase of amplifier noise because it is solely contributed from amplifier noise.

Taking the integration over  $\theta$  and changing the random variable to the received intensity of  $y = r^2$ , we get

$$\mathcal{F}_{\omega}^{-1} \{ \Psi_{\Phi, Y} \} = \frac{\Psi_{\Phi}(\nu)}{2\sigma_{\nu}^2} \exp \left[ -\frac{y + |\vec{\xi}_{\nu}|^2}{2\sigma_{\nu}^2} \right] I_0 \left[ \sqrt{y} \frac{|\vec{\xi}_{\nu}|}{\sigma_{\nu}^2} \right], \quad (26)$$

where  $I_k(\cdot)$  is the  $k^{\text{th}}$ -order modified Bessel function of the first kind. The p.d.f. of the received intensity of

$$p_Y(y) = \mathcal{F}_{\omega}^{-1} \{ \Psi_{\Phi, Y} \} (\nu, y) \Big|_{\nu=0} = \exp(-y - \rho_s) I_0(2\sqrt{y\rho_s}) \quad (27)$$

is a non-central  $\chi^2$ -p.d.f. with two degrees of freedom with a noncentrality parameter of  $\rho_s$  and variance parameter of  $1/2$ .

Taking a Fourier transform of (26), the joint characteristic function of nonlinear phase noise and received intensity is

$$\Psi_{\Phi, Y}(\nu, \omega) = \frac{\Psi_{\Phi}(\nu)}{1 - 2j\omega\sigma_{\nu}^2} \exp \left[ \frac{j\omega|\vec{\xi}_{\nu}|^2}{1 - 2j\omega\sigma_{\nu}^2} \right], \quad (28)$$

or

$$\Psi_{\Phi, Y}(\nu, \omega) = \frac{1}{\cos\sqrt{j\nu} - j\omega\frac{\sin\sqrt{j\nu}}{\sqrt{j\nu}}} \times \exp \left[ \rho_s \sqrt{j\nu} \tan\sqrt{j\nu} + \frac{j\omega\rho_s}{\cos^2\sqrt{j\nu} - j\omega\frac{\sin(2\sqrt{j\nu})}{2\sqrt{j\nu}}} \right]. \quad (29)$$

The joint characteristic function of (29) can be used to study the compensation of nonlinear phase noise using received intensity [5, 6, 7].

### B. Joint Characteristic Function of Nonlinear Phase Noise and Phase of Amplifier Noise

Using the characteristic function of (25), take the integration over the received amplitude  $r$ , we get

$$\mathcal{F}_{\omega}^{-1} \{ \Psi_{\Phi, \Theta_n} \} = \frac{\Psi_{\Phi}(\nu)}{2\pi\sigma_{\nu}^2} \times \int_0^{\infty} \exp \left[ -\frac{r^2 + |\vec{\xi}_{\nu}|^2 - 2r|\vec{\xi}_{\nu}| \cos(\theta - \theta_0)}{2\sigma_{\nu}^2} \right] r dr, \quad (30)$$

or

$$\mathcal{F}_{\omega}^{-1} \{ \Psi_{\Phi, \Theta_n} \} = \Psi_{\Phi}(\nu) \times \left\{ \frac{1}{2\pi} e^{-\gamma\nu} + \sqrt{\frac{\gamma\nu}{4\pi}} \cos(\theta - \theta_0) e^{-\gamma\nu \sin^2(\theta - \theta_0)} \times \operatorname{erfc}[-\sqrt{\gamma\nu} \cos(\theta - \theta_0)] \right\}, \quad (31)$$

where

$$\gamma\nu = \frac{|\vec{\xi}_{\nu}|^2}{2\sigma_{\nu}^2} = \frac{2\sqrt{j\nu}}{\sin(2\sqrt{j\nu})} \rho_s \quad (32)$$

can be interpreted as the angular frequency depending SNR.

Taking the Fourier transform of (31), from [29, §9.2-2], the characteristic function of  $\Psi_{\Phi, \Theta_n}$  is

$$\Psi_{\Phi, \Theta_n}(\nu, \omega) = \Psi_{\Phi}(\nu) \times \sum_{m=0}^{\infty} \epsilon_m \frac{\gamma\nu^{m/2}}{2m!} \Gamma\left(\frac{m}{2} + 1\right) {}_1F_1\left(\frac{m}{2}; m + 1; -\gamma\nu\right) \times \left[ \frac{(e^{2\pi j(m+\omega)} - 1)e^{-jm\theta_0}}{2j\pi(m+\omega)} + \frac{(e^{2\pi j(\omega-m)} - 1)e^{jm\theta_0}}{2j\pi(\omega-m)} \right]. \quad (33)$$

where  $\Gamma(\cdot)$  is the Gamma function,  ${}_1F_1(a; b; \cdot)$  is the confluent hypergeometric function of the first kind with parameters of  $a$  and  $b$ , and  $\epsilon_m = 1$  if  $m = 1$ ,  $\epsilon_m = 2$  if  $m \geq 1$ .

Within the summation of the joint characteristic function of (33), if  $\omega = m$  as an integer, only one term in the summation is non-zero. We have

$$\Psi_{\Phi, \Theta_n}(\nu, m) = \frac{\Psi_{\Phi}(\nu)\gamma\nu^{m/2}}{m!} \Gamma\left(\frac{m}{2} + 1\right) \times {}_1F_1\left(\frac{m}{2}; m + 1; -\gamma\nu\right) e^{jm\theta_0}, \quad m \geq 0, \quad (34)$$

and  $\Psi_{\Phi, \Theta_n}(\nu, -m) = \Psi_{\Phi, \Theta_n}(\nu, m)e^{-2jm\theta_0}$ . The simple expression for  $\Psi_{\Phi, \Theta_n}(\nu, m)$  is very helpful to derive the p.d.f. of the signal phase.

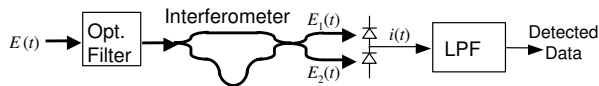


FIG. 4: The direct-detection receiver of DPSK signal using an interferometer.

## V. ERROR PROBABILITY OF DPSK SIGNAL

Binary DPSK signaling with interferometer based direct-detection receiver has renewed interests recently [9, 11, 12, 13, 14]. Optical amplified direct-detection DPSK receiver had been studied by [28, 30, 31]. This section studies the impact of nonlinear phase noise to binary DPSK signal. In order to derive the error probability, the p.d.f. of the received phase, that is the summation of both nonlinear phase noise and the phase of amplifier noise, is first derived analytically.

Fig. 4 shows the direct-detection receiver for DPSK signal. The DPSK receiver uses a Mach-Zehnder interferometer in which the signal is splitted into two paths and combined with a path difference of a symbol time of  $T$ . In practice, the path difference  $\tau \approx T$  must be chosen such that  $\exp(j\omega_0\tau) = 1$ , where  $\omega_0$  is the angular frequency of the signal [32]. Ideally, the optical filter before the interferometer is assumed to be a match filter to the transmitted signal. Two balanced photodetectors are used to receive the photocurrent. There is a low-pass filter to filter out the receiver noise. We assume that the low-pass filter has a wide bandwidth and does not distort the received signal.

The analysis here just takes into account the amplifier noise from the same polarization as the signal [30] and can also be applied to heterodyne receiver [31]. The receiver noise, including shot and thermal noise, is ignored.

### A. Phase Distribution

Without loss of generality, in this section, the normalized transmitted electric field is assumed to be  $\vec{\xi}_0 = (\sqrt{\rho_s}, 0)$  and  $\theta_0 = 0$ . Using the joint characteristic function of (33), the summation of the nonlinear phase noise and the phase of amplifier noise

$$\phi_r = \phi_{\text{NL}} + \theta_n = \frac{\langle \Phi_{\text{NL}} \rangle}{\rho_s + 1/2} \phi + \theta_n \quad (35)$$

has a characteristic function of

$$\Psi_{\phi_r}(\nu) = \Psi_{\phi, \Theta_n} \left( \frac{\langle \Phi_{\text{NL}} \rangle}{\rho_s + 1/2} \nu, \nu \right). \quad (36)$$

While the distribution of the phase of amplifier noise does not change due to the normalization of (3), the distribution of the nonlinear phase noise changes due

to the normalization. In practice, the p.d.f. of the received phase of (35) is a periodic function with a period of  $2\pi$ . With normalization, the normalized nonlinear phase noise of (3) is not limited to  $2\pi$  but scaled up by a large ratio of  $\rho_s + 1/2$  to  $\langle \Phi_{\text{NL}} \rangle$ .

As a periodic function with period of  $2\pi$ , the p.d.f. of the received phase has a Fourier series expansion of

$$p_{\Phi_r}(\theta) = \frac{1}{2\pi} \sum_{m=-\infty}^{+\infty} \Psi_{\Phi_r}(m) \exp(jm\theta) \quad (37)$$

with  $\Psi_{\Phi_r}(m)$  as the Fourier coefficients.

A DPSK signal is demodulated using the differential phase of

$$\begin{aligned} \Delta\Phi_r &= \phi_r(t) - \phi_r(t-T) \\ &= \theta_n(t) - \phi_{\text{NL}}(t) - \theta_n(t-T) + \phi_{\text{NL}}(t-T), \end{aligned} \quad (38)$$

where  $\phi_r(\cdot)$ ,  $\theta_n(\cdot)$ , and  $\phi_{\text{NL}}(\cdot)$  are the received phase, the phase of the amplifier noise, and the nonlinear phase noise as a function of time. The expression of (38) assumes that the signal phases at  $t$  and  $t-T$  are the same. The phases at  $t$  and  $t-T$  are i.i.d. random variables.

In practice, an interferometer based balanced receiver of Fig. 4 gives a photocurrent or voltage proportional to  $\cos(\Delta\Phi_r)$ . The detector makes a decision on whether  $\cos(\Delta\Phi_r)$  is positive or negative. This detector is equivalent to make a decision on whether  $\Delta\Phi_r$  is within or without the angle of  $\pm\pi/2$ . Error probability is calculated using the p.d.f. of the differential phase  $\Delta\Phi_r$ .

The addition or subtraction of two independent random variables is equivalent to the multiplication of the Fourier series coefficients of the corresponding p.d.f. Using the Fourier series of (37), the p.d.f. of the differential phase  $\Delta\Phi_r$  is

$$p_{\Delta\Phi_r}(\theta) = \frac{1}{2\pi} + \frac{1}{\pi} \sum_{m=1}^{+\infty} |\Psi_{\Phi_r}(m)|^2 \cos(m\theta). \quad (39)$$

From (38), the random variable of  $\Delta\Phi_r$  is the difference of two i.i.d. random variables. The p.d.f. for  $\Delta\Phi_r$  is symmetrical with respect to zero. The Fourier coefficients of  $|\Psi_{\Phi_r}(m)|^2$  are real numbers.

Using the Fourier series expansion like (39), the error probability is found for DPSK signals with a noisy reference [18], phase error [33], or laser phase noise [19]. All previous studies [18, 19, 33] had phase noise or error that is independent of the phase of the signal, or using our symbol, the random variable  $\Phi_{\text{NL}}$  is independent of  $\Theta_n$ . Here, the problem is far more complicated because of the dependence between the nonlinear phase noise  $\Phi_{\text{NL}}$  and the phase of amplifier noise of  $\Theta_n$ .

## B. Error Probability

The error probability of DPSK signal with nonlinear phase noise is

$$p_e = 1 - \int_{-\pi/2}^{\pi/2} p_{\Delta\Phi_r}(\theta) d\theta, \quad (40)$$

or

$$p_e = \frac{1}{2} - \frac{1}{\pi} \sum_{m=1}^{\infty} |\Psi_{\Phi_r}(m)|^2 \frac{2 \sin(m\pi/2)}{m}. \quad (41)$$

Because  $\sin(m\pi/2) = 0$  if  $m$  is an even number, we get

$$p_e = \frac{1}{2} - \frac{2}{\pi} \sum_{k=0}^{\infty} \frac{(-1)^k}{2k+1} |\Psi_{\Phi_r}(2k+1)|^2, \quad (42)$$

where, from the expressions of (36) and (34),

$$\begin{aligned} & \Psi_{\Phi_r}(2k+1) \\ &= \frac{\Gamma(k + \frac{3}{2}) \lambda_k^{k+\frac{1}{2}}}{(2k+1)!} {}_1F_1\left(k + \frac{1}{2}; 2k+3; -\lambda_k\right) \\ & \quad \times \Psi_{\Phi} \left[ \frac{(2k+1) \langle \Phi_{NL} \rangle}{\rho_s + 1/2} \right] \\ &= \frac{\sqrt{\pi} \lambda_k}{2} e^{-\lambda_k/2} \left[ I_k \left( \frac{\lambda_k}{2} \right) + I_{k+1} \left( \frac{\lambda_k}{2} \right) \right] \\ & \quad \times \Psi_{\Phi} \left[ \frac{(2k+1) \langle \Phi_{NL} \rangle}{\rho_s + 1/2} \right], \end{aligned} \quad (43)$$

and

$$\lambda_k = \frac{2 \left[ \frac{j(2k+1) \langle \Phi_{NL} \rangle}{\rho_s + 1/2} \right]^{1/2}}{\sin \left\{ 2 \left[ \frac{j(2k+1) \langle \Phi_{NL} \rangle}{\rho_s + 1/2} \right]^{1/2} \right\}} \rho_s. \quad (44)$$

In the coefficients of (43), the conversion from confluent hypergeometric function to Bessel function is used in [18, 33, 34, 35]. The complex coefficients of  $\lambda_k$  (44) are equivalent to the angular frequency depending SNR parameters. Bessel functions with complex argument are well-defined [36].

## C. Approximation of Independence

The coefficients of (43) have a very complicated expression because of the dependence between the phase of amplifier noise and the nonlinear phase noise. Because  $E\{\Theta_n \Phi_{NL}\} = 0$ , the phase of amplifier noise and the nonlinear phase noise are uncorrelated with each other.

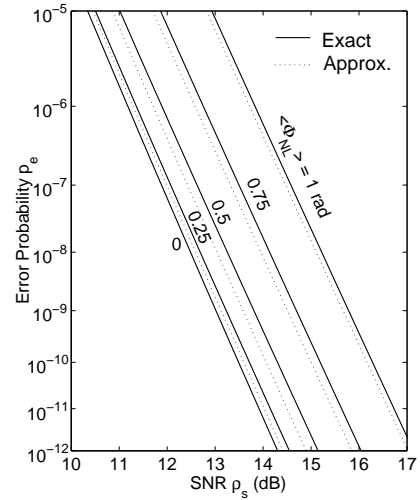


FIG. 5: The exact and approximated error probability as a function of SNR for DPSK signal with nonlinear phase noise.

However, uncorrelated is not equivalent to independence for non-Gaussian random variables.

If the phase of amplifier noise and the nonlinear phase noise is assumed to be independent of each other, the error probability is

$$p_e \approx \frac{1}{2} - \frac{\rho_s e^{-\rho_s}}{2} \sum_{k=1}^{\infty} \frac{(-1)^k}{2k+1} \left[ I_k \left( \frac{\rho_s}{2} \right) + I_{k+1} \left( \frac{\rho_s}{2} \right) \right]^2 \times \left| \Psi_{\Phi} \left[ \frac{(2k+1) \langle \Phi_{NL} \rangle}{\rho_s + 1/2} \right] \right|^2. \quad (45)$$

Similar to the error probability in [18, 19, 33] when phase noise is independent of signal phase, the approximated error probability of (45) is simpler than the exact error probability of (42) with coefficients of (43).

Comparing the exact (42) and approximated (45) error probability, two expressions are the same if the parameter of  $\lambda_k$  (44) in the coefficient of (43) is replaced by the SNR of  $\rho_s$ . The parameter of  $\lambda_k$  is a complex number. With nonlinear phase noise, the absolute value of  $|\lambda_k|$  is always smaller than the SNR  $\rho_s$ . The exact error probability of (42) is always larger than the approximated error probability of (45).

Because of its simple expression, the approximated error probability (45) can be used together with the characteristic functions with finite number of fiber spans [16]. The error probability with and without compensation can be calculated using the approximated error probability of (45).

## D. Numerical Results

Fig. 5 plots the exact (42) and approximated (45) error probability as a function of the SNR for DPSK signal

with nonlinear phase noise. Fig. 5 also gives the error probability of DPSK signal without nonlinear phase noise of [18], [25, §5.2.8], [34]

$$p_e = \frac{\exp(-\rho_s)}{2}. \quad (46)$$

From Fig. 5, the approximated error probability of (45) is always smaller than that of the exact error probability of (42). For the same error probability of  $10^{-9}$ , the difference in terms of SNR is less than 0.2 dB, an insignificant discrepancy for most practical applications. The approximated error probability based on the independence assumption is more accurate if either the nonlinear phase noise or the phase of amplifier noise is the dominant noise source. As shown in Fig. 5, the discrepancy between the exact and approximated error probability is smaller for small or large nonlinear phase noise than, for example, with a mean nonlinear phase shift of  $\langle \Phi_{\text{NL}} \rangle = 0.75$  rad.

The variance of the phase of amplifier noise is approximately equal to  $1/\rho_s$ . The variance of the nonlinear phase noise is approximately equal to  $4 \langle \Phi_{\text{NL}} \rangle^2 \rho_s/3$ . When the mean nonlinear phase shift  $\langle \Phi_{\text{NL}} \rangle$  is about 0.87 rad, the variance of nonlinear phase noise and the phase of amplifier noise are more or less the same. The independence approximation gives the largest discrepancy in a mean nonlinear phase shift from 0.5 to 1 rad.

The error probability of Fig. 5 is calculated using Matlab. The series summation of (42) and (45) can be calculated to an error probability of  $10^{-13}$  to  $10^{-14}$  with an accuracy of three to four significant digits. Symbolic mathematical software can provide better accuracy by using variable precision arithmetic in the calculation of low error probability.

## VI. COMPENSATION OF NONLINEAR PHASE NOISE

As shown in the helix shape scattergram of Figs. 1, nonlinear phase noise is correlated with the received intensity. The received intensity can be used to compensate for nonlinear phase noise. Ideally, the optimal compensator should minimize the error probability of the system after compensation. If the joint p.d.f. of the received phase and the received intensity of  $p_{\Phi_r, Y}(\theta, y)$  is available, the optimal compensator or detector is given by the maximum *a posteriori* probability (MAP) criterion [21, §5.2] to minimize the error probability.

In this section, the compensator is optimized in term of the variance, or mean-square error criterion, of the residual nonlinear phase noise. The optimal compensator is derived with and without the linearity constraint.

### A. Linear Compensation

The simplest method to compensate the nonlinear phase noise is to add a scaled received intensity into the

received phase [5, 6, 7]. The optimal linear compensator minimizes the variance of the normalized residual phase noise of  $\phi_\alpha = \phi - \alpha r^2 = \phi - \alpha y$ . Using the joint characteristic function of (29), the characteristic function for the normalized residual nonlinear phase noise is

$$\Psi_{\Phi_\alpha}(\nu) = \Psi_{\Phi, Y}(\nu, -\alpha\nu). \quad (47)$$

The mean of the normalized residual nonlinear phase noise is

$$\begin{aligned} \langle \Phi_\alpha \rangle &= -j \frac{d}{d\nu} \Psi_{\Phi_\alpha}(\nu) \Big|_{\nu=0} \\ &= \rho_s + \frac{1}{2} - \alpha(\rho_s + 1). \end{aligned} \quad (48)$$

The variance of the normalized residual nonlinear phase noise is

$$\begin{aligned} \sigma_{\Phi_\alpha}^2 &= -j \frac{d^2}{d\nu^2} \Psi_{\Phi_\alpha}(\nu) \Big|_{\nu=0} - \langle \Phi_\alpha \rangle^2 \\ &= \frac{2}{3}\rho_s + \frac{1}{6} - 2\left(\rho_s + \frac{1}{3}\right)\alpha + (2\rho_s + 1)\alpha^2. \end{aligned} \quad (49)$$

Solving  $d\sigma_{\Phi_\alpha}^2/d\alpha = 0$ , the optimal scale factor for linear compensator is

$$\alpha_{\text{opt}} = \frac{1}{2} \frac{\rho_s + 1/3}{\rho_s + 1/2}. \quad (50)$$

In high SNR,  $\alpha_{\text{opt}} \rightarrow 1/2$ . Other than the normalization, the optimal scale factor of (50) is the same as that in [7]. The approximation of  $\alpha_{\text{opt}} \rightarrow 1/2$  was estimated by [6] though simulation.

With the optimal scale factor of (50), the mean and variance of the normalized residual nonlinear phase noise are

$$\langle \Phi_{\alpha_{\text{opt}}} \rangle = \frac{1}{2} \frac{\rho_s^2 + 2\rho_s/3 + 1/6}{\rho_s + 1/2}, \quad (51)$$

$$\sigma_{\Phi_{\alpha_{\text{opt}}}}^2 = \frac{1}{6} \frac{\rho_s^2 + \rho_s + 1/6}{\rho_s + 1/2}. \quad (52)$$

The mean of the residual nonlinear phase noise is about half the mean of the nonlinear phase noise of  $\langle \Phi \rangle$ . The variance of the residual nonlinear phase noise is about a quarter of that of the variance of the nonlinear phase noise of  $\sigma_\Phi^2$ .

After the linear compensation, the characteristic function of the residual normalized nonlinear phase noise is

$$\Psi_{\Phi_{\alpha_{\text{opt}}}}(\nu) = \Psi_{\Phi, Y}\left(\nu, -\frac{\nu}{2} \frac{\rho_s + 1/3}{\rho_s + 1/2}\right). \quad (53)$$

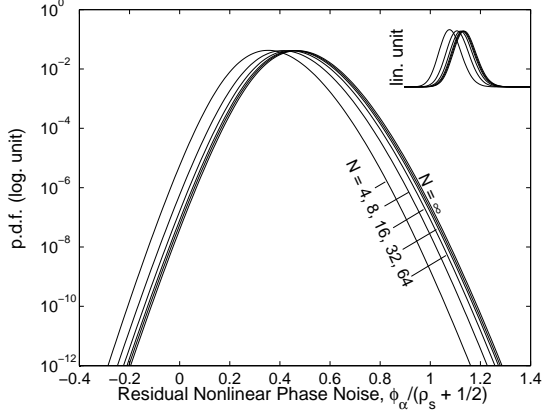


FIG. 6: The asymptotic p.d.f. of the residual nonlinear phase noise  $\phi_\alpha$  as compared with the p.d.f. of  $N = 4, 8, 16, 32$ , and  $64$  fiber spans. The p.d.f. in linear scale is shown in the inset.

The p.d.f. of the residual normalized nonlinear phase noise is the inverse Fourier transform of  $\Psi_{\Phi_{\alpha_{\text{opt}}}}(\nu)$ .

The p.d.f. of the residual nonlinear phase noise for finite number of fiber spans was derived by modeling the residual nonlinear phase noise  $\phi_\alpha$  as the summation of  $N$  independently distributed random variables [16]. Fig. 6 shows a comparison of the p.d.f. for  $N = 4, 8, 16, 32$ , and  $64$  of fiber spans [16] with the distributed case of (53). The residual nonlinear phase noise is scaled by the mean normalized phase shift of  $\langle \Phi \rangle = \rho_s + 1/2$ . Using a SNR of  $\rho_s = 18$ , Fig. 6 is plotted in logarithmic scale to show the difference in the tail. Fig. 6 also provides an inset in linear scale of the same p.d.f. to show the difference around the mean. Like that of Fig. 3, the asymptotic p.d.f. for residual nonlinear phase noise of Fig. 6 is also very accurate for  $N \geq 32$  fiber spans. Unlike that of Fig. 3, the asymptotic p.d.f. for residual nonlinear phase noise of Fig. 6 have slightly larger spread than that of the finite cases. The mean of the residual nonlinear phase noise is about  $0.5(\rho_s + 1/2)$ , the same as that of (51). Comparing Fig. 3 and Fig. 6, with linear compensation, both the mean and STD of the residual nonlinear phase noise is about half of that of the nonlinear phase noise before compensation.

## B. Nonlinear Compensation

The optimal compensator estimates the nonlinear phase using the received intensity by the conditional mean of  $E\{\Phi|R\} = E\{\Phi|Y\} = E\{\Phi|R^2\}$ . The conditional mean is the Bayes estimator that minimizes the variance of the residual nonlinear phase noise without the constraint of linearity [21, §10.2]. We call the estimation of  $E\{\Phi|R\}$  an estimation based on received intensity although it is actually based on received amplitude. To find the conditional mean  $E\{\Phi|R\}$ , either the conditional p.d.f. of  $p_{\Phi|R}$  or the conditional characteristic function of

$\Psi_{\Phi|R}$  is required. The conditional characteristic function of  $\Psi_{\Phi|R}$  can be found using the relationship of

$$\Psi_{\Phi|Y}(\nu|y) = \frac{\mathcal{F}_\omega^{-1}\{\Psi_{\Phi,Y}\}(\nu, y)}{p_Y(y)}. \quad (54)$$

Using (26) and (27), we have

$$\Psi_{\Phi|Y}(\nu|y) = \frac{\Psi_\Phi(\nu)}{2\sigma_\nu^2} \times \frac{\exp\left[-\frac{y+|\xi_\nu|^2}{2\sigma_\nu^2}\right] I_0\left(\sqrt{y}\frac{|\xi_\nu|}{\sigma_\nu^2}\right)}{\exp\left[-(y+\rho_s)\right] I_0\left(2\sqrt{y\rho_s}\right)}. \quad (55)$$

The optimal compensator is the conditional mean of the nonlinear phase noise given the received intensity of  $Y = R^2$ , we get

$$\begin{aligned} E\{\Phi|R\} &= -j \frac{d}{d\nu} \Psi_{\Phi|Y}(\nu|y) \Big|_{\nu=0, y=r^2} \\ &= \frac{1}{6} + \frac{1}{3}\rho_s + \frac{1}{3}r^2 + \frac{\sqrt{\rho_s}r}{3} \frac{I_1(2r\sqrt{\rho_s})}{I_0(2r\sqrt{\rho_s})}. \end{aligned} \quad (56)$$

The residual nonlinear phase noise is  $\phi_e = \phi - E\{\Phi|R\}$ , its conditional variance is

$$\begin{aligned} \sigma_{\Phi_e|R}^2(r) &= -\frac{d^2}{d\nu^2} \Psi_{\Phi|Y}(\nu|y) \Big|_{\nu=0, y=r^2} - E\{\Phi|R\}^2 \\ &= \frac{1+4(\rho_s+r^2)}{90} + \frac{r^2\rho_s}{9} \\ &\quad + \frac{\sqrt{\rho_s}r}{45} \frac{I_1(2r\sqrt{\rho_s})}{I_0(2r\sqrt{\rho_s})} - \frac{r^2\rho_s}{9} \frac{I_1^2(2r\sqrt{\rho_s})}{I_0^2(2r\sqrt{\rho_s})}. \end{aligned} \quad (57)$$

The variance of the residual nonlinear phase noise can be numerically integrated as

$$\sigma_{\Phi_e}^2 = 2 \int_0^\infty \sigma_{\Phi_e|R}^2(r) p_Y(r^2) r dr, \quad (58)$$

where  $p_Y(y)$  is the p.d.f. of the received intensity of (27). Using (26), the characteristic function of the residual nonlinear phase noise can be numerically integrated as

$$\begin{aligned} \Psi_{\Phi_e}(\nu) &= 2 \int_0^\infty \mathcal{F}_\omega^{-1}\{\Psi_{\Phi,Y}\}(\nu, r^2) \\ &\quad \times \exp(-j\nu E\{\Phi|R\}) r dr. \end{aligned} \quad (59)$$

The p.d.f. of the residual nonlinear phase noise is the inverse Fourier transform of the characteristic function of (59).

## C. Comparison of Linear and Nonlinear Compensators

Fig. 7 plots the compensation curves of linear and nonlinear compensator for SNR of  $\rho_s = 11, 18$ , and  $25$ . The

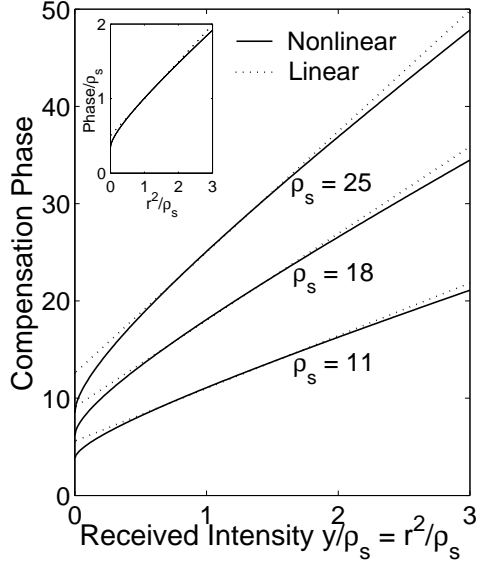


FIG. 7: The compensation curves of linear and nonlinear compensators.

linear compensation curve is  $\langle \Phi_{\alpha_{\text{opt}}} \rangle + \alpha_{\text{opt}} r^2$ . The nonlinear compensation curve is  $E\{\Phi|R\}$  of (56). In Fig. 7, the received intensity of  $y = r^2$  is scaled by the corresponding SNR of  $\rho_s$  but the compensation phase is not scaled. The inset also shows the corresponding curves when both compensation phase and the received intensity are scaled by the corresponding SNR of  $\rho_s$ , giving three almost overlapped curves. From Fig. 7, when the normalized received intensity is between  $0.5\rho_s$  to  $2\rho_s$ , the linear and nonlinear compensators have almost no difference. Because the mean normalized received intensity is  $\rho_s + 1$ , the linear and nonlinear compensators are almost the same when the intensity is between half and twice the mean of the received intensity. When the received intensity is either beyond the range of  $0.5\rho_s$  or  $2\rho_s$ , the nonlinear compensator always gives a smaller compensation phase than that of the linear compensator. In the scaled inset, all the curves have a slope of about  $1/2$ .

Fig. 8 plots the standard deviation (STD) of the normalized nonlinear phase noise with and without compensation as a function of SNR  $\rho_s$ . The STD of residual nonlinear phase noise of  $\sigma_{\Phi_{\alpha_{\text{opt}}}}$  and  $\sigma_{\Phi_e}$ , with linear and nonlinear compensator, are shown as almost overlapped solid and dotted lines, respectively. The STD of nonlinear compensator is about 0.2% less than that of linear compensator. In term of the variance or STD of the residual nonlinear phase noise, Fig. 8 shows that the optimal nonlinear compensator has the same performance as the linear compensator. The variance of the residual nonlinear phase noise is contributed mostly from the region when the nonlinear phase noise is around its mean of  $\rho_s + 1/2$ . As from Fig. 7, the linear and nonlinear compensation curves have no significant difference from  $0.5\rho_s$  to  $2\rho_s$ . The variance of the residual nonlinear phase should

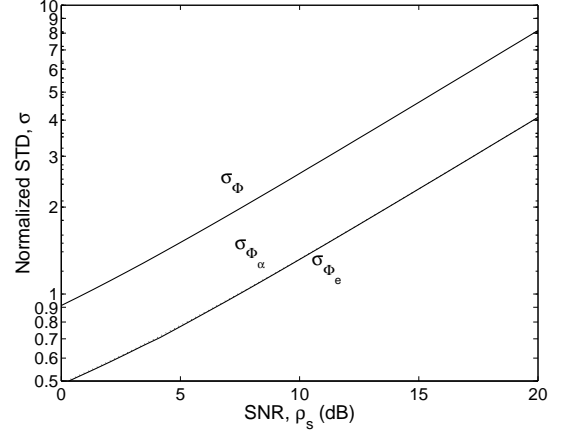


FIG. 8: The STD of normalized nonlinear phase noise with and without compensation.

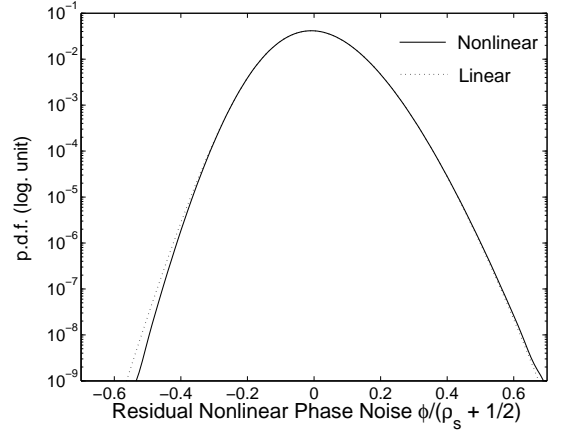


FIG. 9: The p.d.f. of the residual nonlinear phase noise with linear and nonlinear compensation.

have no significant difference whether linear or nonlinear compensator is used.

Fig. 9 compares the p.d.f. of the residual nonlinear phase noise with linear and nonlinear compensation. The residual nonlinear phase noise is scaled by the mean normalized nonlinear phase shift of  $\langle \Phi \rangle = \rho_s + 1/2$ . The asymptotic p.d.f. with linear compensator of Fig. 6 is reproduced in Fig. 9 and shifted by the mean of  $\langle \Phi_{\alpha_{\text{opt}}} \rangle$  of (51), giving a better comparison to the residual nonlinear phase with nonlinear compensator.

If Fig. 9 is plotted in linear scale, the two p.d.f. curves overlap. The major difference of the p.d.f. is at the tail of the negative phase. The p.d.f. using the nonlinear compensator has a smaller tail probability than that of linear compensator if the phase is less than  $-0.4(\rho_s + 1/2)$ . Although the small discrepancy at the tail does not affect the variance of Fig. 8, nonlinear compensator provides smaller error probability than that of linear compensator. Comparing Fig. 8 and Fig. 9, the variance of residual nonlinear phase noise is useful but may not be the only criterion to characterize the performance of the

compensation scheme.

The approximated error probability of (45) can be used with the characteristic function of residual nonlinear phase noise after linear or nonlinear compensator of  $\Psi_{\Phi_{\alpha_{\text{opt}}}}(\nu)$  (53) and  $\Psi_{\Phi_e}(\nu)$  (59), respectively. While the residual nonlinear phase noise may slightly depend on the phase of amplifier noise, the dependence is weak and may be ignored.

## VII. CONCLUSION

The joint characteristic functions of the nonlinear phase noise with electric field, received intensity, and the phase of amplifier noise are derived analytically the first time. The nonlinear phase noise is modeled asymptotically as a distributed process for large number of fiber spans. Replacing the span by span summation of the nonlinear phase noise by an integration, the distributed

assumption is valid if the number of fiber spans is larger than 32. Using the joint characteristic function of the nonlinear phase noise with the phase of amplifier noise, the error probability of DPSK signal is calculated as a series. The error probability of DPSK signal is simplified by assuming that the nonlinear phase noise is independent of the phase of amplifier noise. When the received intensity is used to compensate the nonlinear phase noise, based on the principle to minimize the variance of the residual nonlinear phase noise, the optimal linear and nonlinear compensators are derived analytically using the joint characteristic function of the nonlinear phase noise with the received intensity. While the residual nonlinear phase noise of both linear and nonlinear compensators has the almost same variance, the tail probability of the residual nonlinear phase noise of nonlinear compensator is smaller than that of linear compensator, leading to smaller error probability.

- 
- [1] J. P. Gordon and L. F. Mollenauer, *Opt. Lett.* **15**, 1351 (1990).
- [2] S. Ryu, *J. Lightwave Technol.* **10**, 1450 (1992).
- [3] S. Saito, M. Aiki, and T. Ito, *J. Lightwave Technol.* **11**, 331 (1993).
- [4] C. J. McKinstrie and C. Xie, *IEEE J. Sel. Top. Quantum Electron.* **8**, 616 (2002), correction **8**, 956 (2002).
- [5] X. Liu, X. Wei, R. E. Slusher, and C. J. McKinstrie, *Opt. Lett.* **27**, 1616 (2002).
- [6] C. Xu and X. Liu, *Opt. Lett.* **27**, 1619 (2002).
- [7] K.-P. Ho and J. M. Kahn, physics/0211097.
- [8] H. Kim and A. H. Gnauck, *IEEE Photon. Technol. Lett.* **15**, 320 (2003).
- [9] A. H. Gnauck, G. Raybon, S. Chandrasekhar, J. Leuthold, C. Doerr, L. Stulz, A. Agrawal, S. Banerjee, D. Grosz, S. Hunsche, et al., in *Proc. OFC '02* (2002), postdeadline paper FC2.
- [10] R. A. Griffin, R. I. Johnstone, R. G. Walker, J. Hall, S. D. Wadsworth, K. Berry, A. C. Carter, M. J. Wale, P. A. Jerram, and N. J. Parsons, in *Proc. OFC '02* (2002), postdeadline paper FD6.
- [11] B. Zhu, L. Leng, A. H. Gnauck, M. O. Pedersen, D. Peckham, L. E. Nelson, S. Stulz, S. Kado, L. Gruner-Nielsen, R. L. Lingle, et al., in *Proc. ECOC '03* (2002), postdeadline paper PD4.2.
- [12] Y. Miyamoto, H. Masuda, A. Hirano, S. Kuwahara, Y. Kisaka, H. Kawakami, M. Tomizawa, Y. Tada, and S. Aozasa, *Electron. Lett.* **38**, 1569 (2002).
- [13] H. Bissessur, G. Charlet, E. Gohin, C. Simonneau, L. Pierre, and W. Idler, *Electron. Lett.* **39**, 192 (2003).
- [14] A. H. Gnauck, G. Raybon, S. Chandrasekhar, J. Leuthold, C. Doerr, L. Stulz, and E. Burrows, *IEEE Photon. Technol. Lett.* **15**, 467 (2003).
- [15] P. S. Cho, V. S. Grigoryan, Y. A. Godin, A. Salamon, and Y. Achiam, *IEEE Photon. Technol. Lett.* **15**, 473 (2003).
- [16] K.-P. Ho, submitted to *J. Opt. Soc. Amer. B*, physics/0301018.
- [17] K.-P. Ho, submitted to *Opt. Lett.*, physics/0301067.
- [18] P. C. Jain, *IEEE Trans. Info. Theory* **IT-20**, 36 (1974).
- [19] G. Nicholson, *Electron. Lett.* **20**, 1005 (1984).
- [20] C. Xu, L. F. Mollenauer, and X. Liu, *Electron. Lett.* **38**, 1578 (2002).
- [21] R. N. McDonough and A. D. Whalen, *Detection of Signals in Noise* (Academic Press, San Diego, 1995), 2nd ed.
- [22] S. Norimatsu, K. Iwashita, and K. Noguchi, *IEEE Photon. Technol. Lett.* **4**, 765 (1992).
- [23] A. Papoulis, *Probability, Random Variables, and Stochastic Processes* (McGraw Hill, New York, 1984), 2nd ed.
- [24] I. S. Gradshteyn and I. M. Ryzhik, *Table of Integrals, Series, and Products* (Academic Press, San Diego, 1980).
- [25] J. G. Proakis, *Digital Communications* (McGraw Hill, New York, 2000), 4th ed.
- [26] G. J. Foschini and C. D. Poole, *J. Lightwave Technol.* **9**, 1439 (1991).
- [27] C. D. Poole, J. H. Winters, and J. A. Nagel, *Opt. Lett.* **16**, 372 (1991).
- [28] P. A. Humblet and M. Azizoglu, *J. Lightwave Technol.* **9**, 1576 (1991).
- [29] D. Middleton, *An Introduction to Statistical Communication Theory* (McGraw-Hill, New York, 1960).
- [30] S. R. Chinn, D. M. Boroson, and J. C. Livas, *J. Lightwave Technol.* **14**, 370 (1996).
- [31] O. K. Tonguz and R. E. Wagner, *IEEE Photon. Technol. Lett.* **3**, 835 (1991).
- [32] R. S. Vodhanel, A. E. Elrefaie, M. Z. Iqbal, R. E. Wagner, J. L. Gimlett, and S. Tsuji, *J. Lightwave Technol.* **8**, 1379 (1990).
- [33] N. M. Blachman, *IEEE Trans. Commun.* **COM-29**, 364 (1981).
- [34] P. C. Jain and N. M. Blachman, *IEEE Trans. Info. Theory* **IT-19**, 623 (1973).
- [35] N. M. Blachman, *IEEE Trans. Info. Theory* **34**, 1401 (1988).
- [36] D. E. Amos, *ACM Trans. on Math. Software* **12**, 265

(1986).